its name and has been well-documented with diverse plant pathogens, or the conservation of *EDS1* genes in monocotyledonous plants that do not possess TIR-NB-LRR genes.

Multiple TIR-NB-LRR resistance proteins guarding EDS1 can also explain cross-talk in TIR-NB-LRR signaling. The guard model of resistance protein specificity and indirect effector recognition was first substantiated with RIN4, a host protein targeted by the three sequence-unrelated effectors AvrRpm1, AvrB and AvrRpt2, and guarded by the CC-NB-LRR proteins RPM1 and RPS2 (*6*). Interestingly, it was shown that AvrRpm1 in the absence of its canonical resistance protein RPM1 can activate RPS2 in *RIN4 RPS2 rpm1* plants, presumably because RIN4 is a common target of these effectors (*27*).

A new element in the EDS1 guard complex is SRFR1, genetically a negative regulator of TIR-NB-LRR resistance protein-mediated immunity. SRFR1 is likely to localize EDS1-resistance protein interactions to a microsomal compartment. Either by interacting with the resistance protein co-chaperone SGT1 (*18*) or by directly affecting the stability of EDS1-resistance protein complexes shown here, SRFR1 could set a threshold at which resistance proteins are activated, thus regulating resistance protein specificity. In the absence of SRFR1, EDS1-resistance protein complexes would be more easily perturbed by any effector targeting EDS1, resulting in increased cross-talk between TIR-NB-LRR proteins.

We propose that disruption by AvrRps4 of EDS1-RPS4 interactions at a cytoplasmic membrane, where RPS4 is predominantly found at resting state (*13*), constitutes the very first step in RPS4 activation. None of these interactors are integral membrane proteins. Interestingly, Heidrich *et al*. (*28*) observe that activated RPS4 together with EDS1 is predominantly found in the soluble cytoplasmic fraction. In the nucleus, EDS1 was also found to interact with AvrRps4 and RPS4. Furthermore, Heidrich *et al*. (*28*) show that similar to RPS4 and EDS1 (*13*, *20*), AvrRps4 needs to be nuclear-localized for full immunity activation. A function of effector-triggered immunity activation is therefore likely to include alteration of protein complexes to generate a mobile signal to the nucleus. Which of the many TIR-NB-LRR proteins directly interact with EDS1 and how effectors eventually activate immune responses in the nucleus remains to be established.

References and Notes

1. F. L. Takken, W. I. Tameling, *Science* **324**, 744 (2009).
2. M. Todesco *et al*., *Nature* **465**, 632 (2010).
3. T. Boller, S. Y. He, *Science* **324**, 742 (2009).
4. A. F. Bent, D. Mackey, *Annu. Rev. Phytopathol.* **45**, 399 (2007).
5. S. T. Chisholm, G. Coaker, B. Day, B. J. Staskawicz, *Cell* **124**, 803 (2006).
6. P. N. Dodds, J. P. Rathjen, *Nat. Rev. Genet.* **11**, 539 (2010).
7. J. D. Jones, J. L. Dangl, *Nature* **444**, 323 (2006).
8. Y. Belkhadir, R. Subramaniam, J. L. Dangl, *Curr. Opin. Plant Biol.* **7**, 391 (2004).
9. N. Aarts *et al*., *Proc. Natl. Acad. Sci. U.S.A.* **95**, 10306 (1998).
10. A. Falk *et al*., *Proc. Natl. Acad. Sci. U.S.A.* **96**, 3292 (1999).
11. M. Wiermer, B. J. Feys, J. E. Parker, *Curr. Opin. Plant Biol.* **8**, 383 (2005).
12. Q. H. Shen, P. Schulze-Lefert, *EMBO J.* **26**, 4293 (2007).
13. L. Wirthmueller, Y. Zhang, J. D. Jones, J. E. Parker, *Curr. Biol.* **17**, 2023 (2007).
14. Z. Zhu *et al*., *Proc. Natl. Acad. Sci. U.S.A.* **107**, 13960 (2010).
15. S. H. Kim, S. I. Kwon, D. Saha, N. C. Anyanwu, W. Gassmann, *Plant Physiol.* **150**, 1723 (2009).
16. S. I. Kwon, S. H. Kim, S. Bhattacharjee, J. J. Noh, W. Gassmann, *Plant J.* **57**, 109 (2009).
17. S. H. Kim *et al*., *PLoS Pathog.* **6**, e1001172 (2010).
18. Y. Li *et al*., *PLoS Pathog.* **6**, e1001111 (2010).
19. Materials and methods are available as supporting material on *Science* Online.
20. A. V. García *et al*., *PLoS Pathog.* **6**, e1000970 (2010).
21. B. J. Feys, L. J. Moisan, M. A. Newman, J. E. Parker, *EMBO J.* **20**, 5400 (2001).
22. B. J. Feys *et al*., *Plant Cell* **17**, 2601 (2005).
23. J. M. Liu, J. M. Elmore, Z. J. Lin, G. Coaker, *Cell Host Microbe* **9**, 137 (2011).
24. S. Rietz *et al*., *New Phytol.* **191**, 107 (2011).
25. F. Katagiri, K. Tsuda, *Mol. Plant Microbe Interact.* **23**, 1531 (2010).
26. R. A. van der Hoorn, S. Kamoun, *Plant Cell* **20**, 2009 (2008).
27. M. G. Kim, X. Geng, S. Y. Lee, D. Mackey, *Plant J.* **57**, 645 (2009).
28. K. Heidrich *et al*., *Science* **334**, 1401 (2011).
29. K. H. Sohn, Y. Zhang, J. D. Jones, *Plant J.* **57**, 1079 (2009).

Acknowledgments: We thank J. Parker for providing seed of *eds1-2* and *EDS1-YFP* plants, F. Gao and J. C. Nam for technical assistance, and the University of Missouri Molecular Cytology Core for assistance with confocal fluorescence microscopy. This work was supported by the NSF Integrative Organismal Systems Program (grants IOS-0715926 and IOS-1121114) (W.G.).

Supporting Online Material

www.sciencemag.org/cgi/content/full/334/6061/1405/DC1
Materials and Methods
Figs. S1 to S8
Table S1
References (*30*–*35*)

22 July 2011; accepted 25 October 2011
10.1126/science.1211592

The Competitive Advantage of a Dual-Transporter System

Sagi Levy,* Moshe Kafri,* Miri Carmi, Naama Barkai†

Cells use transporters of different affinities to regulate nutrient influx. When nutrients are depleted, low-affinity transporters are replaced by high-affinity ones. High-affinity transporters are helpful when concentrations of nutrients are low, but the advantage of reducing their abundance when nutrients are abundant is less clear. When we eliminated such reduced production of the *Saccharomyces cerevisiae* high-affinity transporters for phosphate and zinc, the elapsed time from the initiation of the starvation program until the lack of nutrients limited growth was shortened, and recovery from starvation was delayed. The latter phenotype was rescued by constitutive activation of the starvation program. Dual-transporter systems appear to prolong preparation for starvation and to facilitate subsequent recovery, which may optimize sensing of nutrient depletion by integrating internal and external information about nutrient availability.

Maintaining nutrient homeostasis is critical to all cells and in particular to microorganisms, whose environment fluctuates in unpredictable ways. A recurrent design in systems that maintain nutrient homeostasis involves switching between transporters of different affinities. High-affinity transporters are used in limiting conditions, but their abundance is decreased in cells growing in conditions where nutrients are abundant (*1*–*14*). Under these conditions, nutrients are transported by low-affinity transporters, although in principle, high-affinity transporters could function equally well. One possible advantage of this switching is a reduction in the load of protein production. However, we found that mass production of high-affinity transporters in yeast had a marginal effect on fitness in rich media (fig. S1). We therefore explored whether this motif has an additional, perhaps regulatory role in maintaining nutrient homeostasis.

Cells can sense nutrient availability with transmembrane receptors, in which case the external nutrient concentration is monitored. This strategy provides indirect information about the internal pools, which are also influenced by growth rate or availability of other nutrients (*15*). Alternatively, cells can directly monitor the internal nutrient concentration and activate the starvation response only when internal pools are depleted (*13*, *16*–*19*). In the latter case, the dual-transporter motif may play a role in signaling nutrient starvation and specifically in prolonging the time window between the initiation of the starvation response and the onset of growth limitation (the "preparation phase").

To see this, consider a cell that uses a single transporter type and assume that nutrient is gradually depleted from the medium, either through consumption by the cells or loss by diffusion

Department of Molecular Genetics, Weizmann Institute of Science, Rehovot 76100, Israel.

*These authors contributed equally to this work.
†To whom correspondence should be addressed. E-mail: naama.barkai@weizmann.ac.il

(Fig. 1, A and B). Initially, a decrease in external nutrient concentration does not affect the internal pools, because the transporters function at maximal velocity. Internal nutrient abundance begins to decrease only when the external concentrations are close to the dissociation constant of the transporters. Notably, this reduction activates the starvation response, and, shortly after, a lack of nutrients begins to limit growth. Therefore, in a system that relies on a single transporter type, the preparation phase is rather short.

A dual-transporter system prolongs the time window between the initiation of the starvation response and the onset of limitation (Fig. 1C): The starvation response is still induced when the concentration of external nutrient is comparable to the dissociation constant of the low-affinity transporters. However, because the high-affinity transporters are produced as part of the starvation response, growth limitation ensues only when nutrient decreases further to approximately the dissociation constant of the high-affinity transporters. The dual-transporter motif thus provides the cells with a prolonged time window in which the starvation response has been activated, but the intracellular nutrient pools are still sufficient for optimal growth. We hypothesized that this advanced preparation may be beneficial when nutrient levels fluctuate, as foreseeing future conditions may facilitate cellular adaptation (*20*, *21*).

We tested these ideas in two well-studied models: phosphate and zinc homeostasis in budding yeast (*3*, *9*, *13*, *16*, *22*). In both systems, production of high-affinity transporters (Pho84 and Zrt1, respectively) is low in rich media, but these transporters accumulate by more than two orders of magnitude as part of the starvation response (Fig. 2A). Cells directly monitor the internal concentrations of phosphate and zinc: Zap1, the transcription factor activating the zinc starvation response, is directly inhibited by zinc (*17*, *19*), whereas Pho4, the transcription factor activating the phosphate starvation response, is regulated by internal phosphate concentration (*13*, *16*, *18*). We predicted that preventing the repression of *PHO84* and *ZRT1* in rich medium would shorten the respective preparation phases.

We replaced the endogenous promoters of the high-affinity transporters for phosphate and zinc by the promoters of *TDH3* or *TEF1*, two genes expressed at high levels in both rich and poor media. The resulting constitutive strains, PHO84^{C} and ZRT1^{C}, express the high-affinity transporters in amounts comparable to the amount of the endogenous proteins in starved cells (Fig. 2A). We incubated wild-type and constitutive cells in media with intermediate nutrient concentrations and monitored the temporal induction of the starvation response with fluorescence reporters: Yellow fluorescent protein (YFP) fused to the *PHO84* promoter was used to monitor the phosphate starvation response, whereas mCherry fused to the *ZRT1* promoter was used to monitor the zinc starvation program (Fig. 2, B and C). The phosphate starvation program was further monitored by profiling gene expression (Fig. 2D). Wild-type cells induced the starvation response over a period of 5.5 hours (phosphate) or 2 hours (zinc) before the cells constitutively expressing the high-affinity transporters did so. During this period, both the wild-type and modified cells grew rapidly at practically the same rate as they did in rich medium (fig. S3, C and D). For the phosphate system, we also characterized the preparation phase in continuous cultures (Fig. 2E). Wild-type cells fully induced the PHO84-YFP reporter when phosphate concentration was below ~400 μM, a concentration comparable to the dissociation constant of the low-affinity transporter [~220 μM (*13*)], whereas cells constitutively expressing the high-affinity transporters fully induced the reporter only at ~60 μM. In both strains, growth limitation was observed only when phosphate concentration was below ~5 μM (our detection limit), a concentration comparable to the dissociation constant of the high-affinity transporter [~9 μM (*13*)] (Fig. 2, F and G, and fig. S2). We conclude that preventing the expression of high-affinity transporters in rich media enables early induction of the starvation response.

Early induction of the starvation response could enhance the fitness of cells in two complementary ways. First, it could prolong growth in the limiting condition. Second, a regulated entry into starvation could facilitate the recovery from starvation once nutrient is replenished. Rapid resumption of growth once nutrient becomes available would provide yeast cells with a strong selection advantage. We therefore compared the recovery from prolonged phosphate or zinc starvation of wild-type cells and cells that constitutively express the high-affinity transporters. Constitutive expression of Pho84 prolonged the recovery from phosphate starvation, whereas constitutive expression of Zrt1 prolonged the recovery from zinc starvation (Fig. 3A and fig. S3A). The effect was specific: Constitutive expression of Zrt1 did not prolong the recovery from phosphate starvation, and constitutive expression of Pho84 did not prolong (indeed, it accelerated) the recovery from zinc starvation. Neither strain was impaired in recovery from glucose starvation (Fig. 3A and fig. S3A).

To better quantify the recovery of the two strains, we used a sensitive competition assay. Wild-type and constitutive cells were differentially labeled using GFP or mCherry markers driven by the constitutive promoter of the *TEF2* gene. We grew the wild-type and modified cells together in the same tube and measured the relative fraction of each strain in the population at

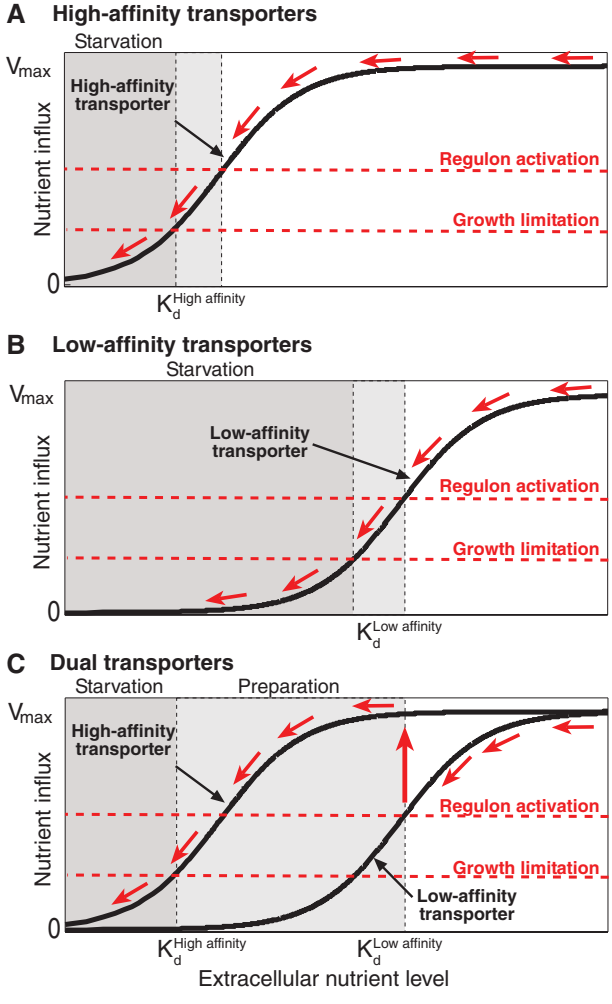

Fig. 1. A dual-transporter system enables advanced preparation for nutrient depletion. (**A**) Nutrient uptake by high-affinity transporters. The flux of incoming nutrient is shown as a function of the external nutrient concentration. The flux decrease upon nutrient depletion is shown with red arrows. The internal nutrient pools follow this flux and are therefore depleted only when external nutrient concentration decreases to below a dissociation constant, $K_d^{High\ affinity}$. Activation of the starvation response occurs at this range (regulon activation), as does growth limitation. (**B**) Nutrient uptake by low-affinity transporters. Same as (A), except with a higher dissociation constant. (**C**) A dual-transporter system prolongs preparation. In a dual-transporter system, activation of the starvation response occurs at ~$K_d^{Low\ affinity}$ (red arrows), whereas growth limitation is reached only when external nutrient is further reduced to ~$K_d^{High\ affinity}$.

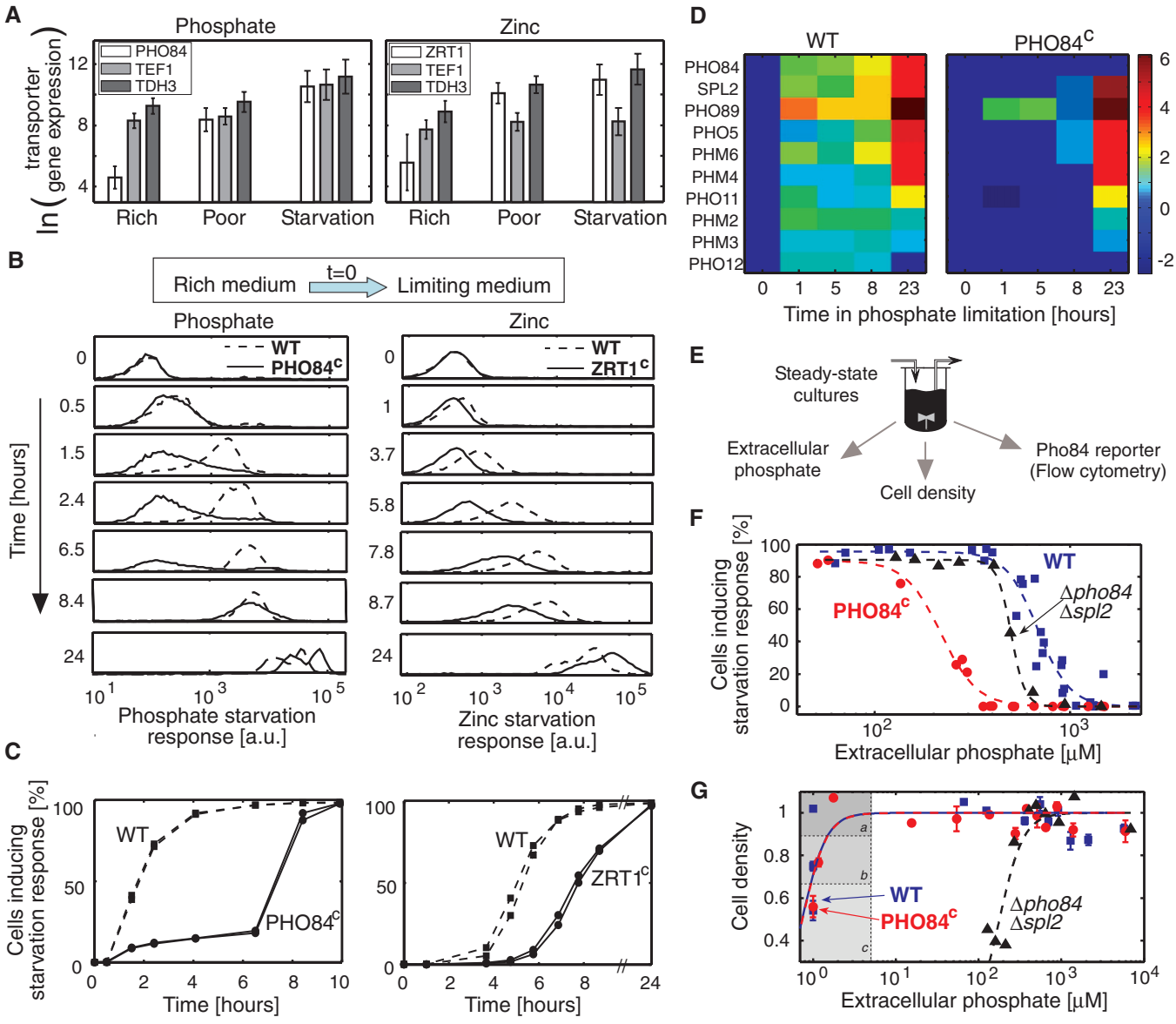

Fig. 2. Constitutive expression of high-affinity transporters shortens preparation. (**A**) Constitutive expression. The constitutive promoters (*TDH3* and *TEF1*) were compared to the endogenous ones (*PHO84* or *ZRT1*) using a fluorescence reporter. Shown are the mean fluorescence during logarithmic growth in rich medium (synthetic complete), poor medium (initial levels of 0.5 mM phosphate or 10 μM zinc), or prolonged starvation (3 days in no-phosphate or no-zinc media), as indicated. Error bars denote variation within the cell population (SD). The increase in protein abundance and protein subcellular localization were verified by constitutive expression of YFP-fused transporters (figs. S6 and S7). This fusion may reduce protein activity, as monitored by slow growth of ZRT1-YFP cells at low zinc; therefore, all experiments were performed with native zinc and phosphate transporters. (**B** and **C**) Delayed starvation response in cells with abundant high-affinity transporters. Wild-type (WT) and constitutive cells ($PHO84^C$ or $ZRT1^C$) were transferred to medium containing low concentrations of phosphate (180 μM, left) or zinc (10 μM, right), respectively. Activation of the starvation program was quantified by following the fluorescence of two reporters: YFP driven by the *PHO84* promoter for monitoring the phosphate starvation response, or mCherry driven by the *ZRT1* promoter for monitoring the zinc starvation response. The single-cell distribution of reporter activation is shown in (B), with the time course summarized in (C) for two biological repeats (cutoff value = 1500 a.u.). Note that wild-type and constitutive cells grow at the same rate (fig. S3, C and D, "Entry," black bars at left). (**D**) Delayed activation of the battery of phosphate-responsive genes. The experiment in (B) and (C) was repeated, with cells transferred to a medium containing 0.5 mM phosphate. The activation of starvation response was measured using microarrays for wild-type and $PHO84^C$ cells. Values are $\log_2$ ratios, the reference being cells grown in rich media. (**E** to **G**) Response to phosphate depletion in continuous cultures. Cells were grown in a chemostat with different concentrations of phosphate in the feeding vessel. The steady-state level of phosphate in the chemostat was quantified using standard assays (*23*), and the activation of the phosphate starvation response was monitored by flow cytometry analysis of the PHO84-YFP reporter. Experiments were repeated for wild-type cells (blue squares), $PHO84^C$ constitutive strains (red circles), and cells expressing only low-affinity transporters (Δ*pho84*Δ*spl2*, black triangles). (**F**) Activation of the starvation response: The fraction of cells activating the starvation response is shown as a function of the phosphate level in the chemostat. See also fig. S2 showing the bistable activation pattern. Lines were added to guide the eye (*23*). (**G**) Effect of phosphate concentration on cell density. Normalized cell density is shown as a function of phosphate concentration in the chemostat. The shaded regions correspond to phosphate concentrations that are below our detection limit of 5 μM. The drop in cell density in low phosphate levels correlates with the reduction of the concentration of phosphate at the feeding vessel of the chemostat (shaded regions a, b, and c correspond to feeding levels of 0.4, 0.3, and 0.2 mM, respectively). Error bars denote SE between biological repeats, when available. Lines were added to guide the eye (*23*) (fig. S2). Constitutive strains in (B) to (G) were driven by *TDH3* promoter.

different time points by flow cytometry (Fig. 3, B and C, and fig. S3, B to D). The cells were transferred into intermediate nutrient conditions where they consumed the nutrients, reached growth limitation, and were transferred back to rich or intermediate nutrient conditions. Consistent with their delayed recovery, the strains constitutively expressing the high-affinity transporters were outcompeted during recovery. Their number in the population rapidly decayed after the transfer to medium rich in nutrient (Fig. 3, B and C, and fig. S3, B to D). The effect was specific: The PHO84^C cells, which were rapidly outcompeted by wild-type cells upon recovery from phosphate limitation, had enhanced recovery from zinc limitation, and the analogous behavior was observed for the ZRT1^C cells. Thus, the constitutive expression of high-affinity transporters appears to limit recovery from starvation of the respective nutrients.

To control for possible effects of toxicity, we repeated the experiments in cells that constitutively expressed the low-affinity transporters for phosphate (Pho90) or zinc (Zrt2). The per-transporter flux is higher for the low-affinity transporters than for the high-affinity ones in both the zinc and phosphate systems (*23*), so we expected that this constitutive expression would exacerbate any toxic effect (see, e.g., fig. S4). However, during entry or exit from starvation, the PHO90^C and ZRT2^C cells grew as well as the wild type (Fig. 3, B and C, and fig. S3, B to D). We conclude that the impaired recovery of the high-affinity constitutive strains, PHO84^C and ZRT1^C, is not likely to be caused by toxicity.

In addition to the delayed recovery from starvation, ZRT1^C cells were outcompeted, although to a lesser extent, while growing in medium with intermediate concentration of zinc until concentration that caused growth limitation (Fig. 3B and fig. S3C). A similar phenotype was observed for PHO84^C, but only when the cells were inoculated directly into a medium containing low concentration of phosphate (0.1 mM; fig. S3C). PHO84^C grew as well as the wild type when incubated in media containing intermediate concentration of phosphate (0.2 mM or 0.5 mM; Fig. 3B and fig. S3C), although they depleted phosphate from

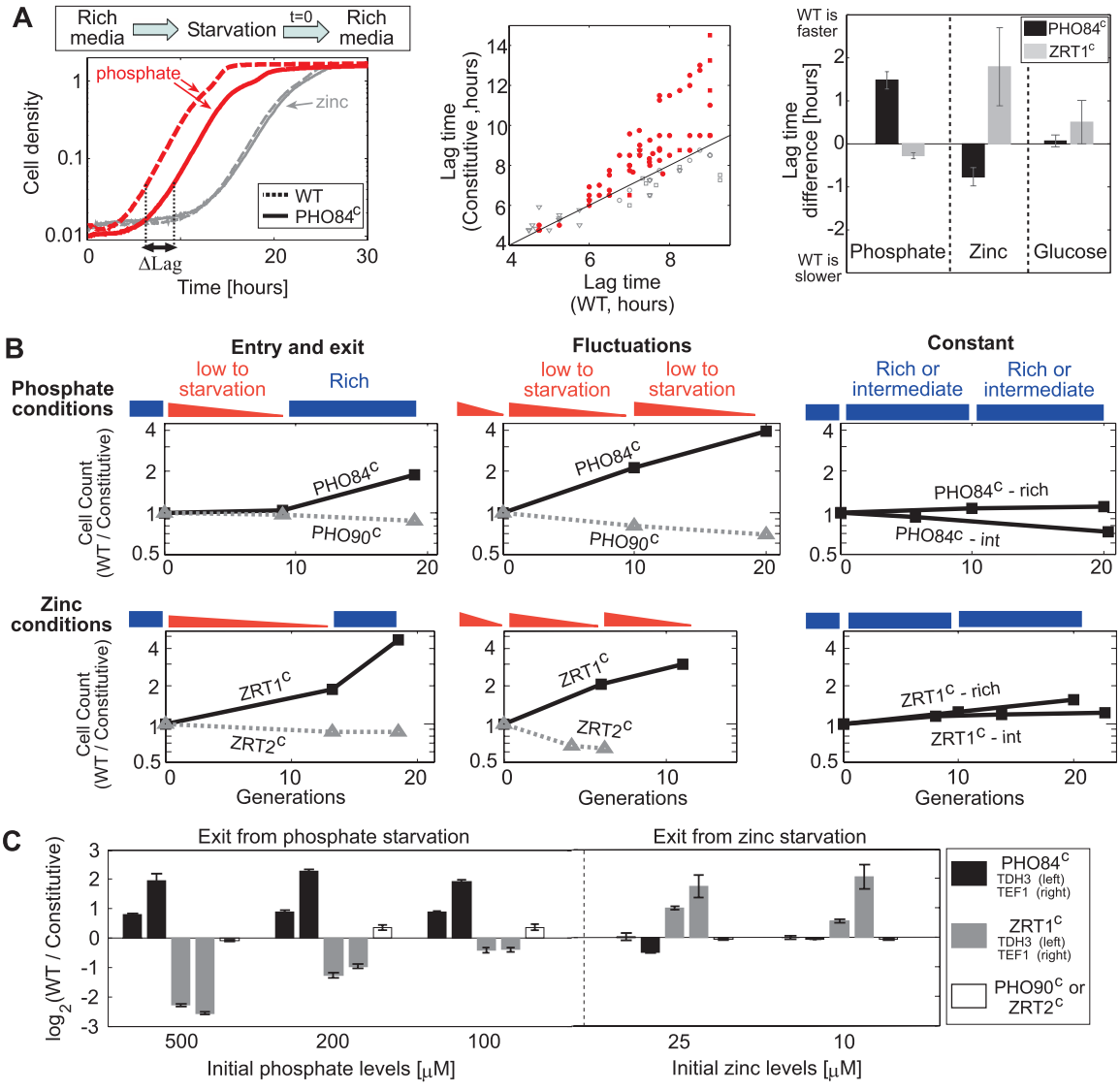

Fig. 3. Impaired recovery from nutrient limitation in cells constitutively expressing high-affinity transporters. (**A**) Recovery from starvation. Cells were deprived of the indicated nutrient and then transferred back to rich medium. The increase in cell density after the transfer is shown. Left: wild-type (dashed) and PHO84^C (solid) cells during recovery from phosphate (red) or zinc (gray) starvation. Center: Lag time of constitutive and wild-type strains. Each point represents a single experiment, differing by the number of days the cells were starved before recovery. Starvation of the relevant nutrient is shown in red (circles, PHO84^C in phosphate; squares, ZRT1^C in zinc), and to nonrelevant nutrients in gray (circles, PHO84^C in zinc; squares, ZRT1^C in phosphate; triangles, PHO84^C or ZRT1^C in glucose). Right: Lag time difference for the conditions and strains indicated. Data are means ± SEM. See fig. S3A for additional controls and detailed results for different constitutive promoters; see table S3 for number of repeats. (**B**) Competition in fluctuating nutrient conditions, shown as the fraction of wild-type to constitutive cells during competitive growth in the conditions indicated. The following conditions were used: entry and exit, initial intermediate levels of 0.5 mM phosphate (P_i) or 10 μM zinc (Zn); fluctuations, initial intermediate levels of 0.5 mM P_i or 25 μM Zn; constant, rich levels of 20 mM P_i or 1500 μM Zn and intermediate levels (with cells kept in logarithmic phase) of 0.5 mM P_i or 300 μM Zn. The constitutive strains presented here are driven by *TDH3* promoter, except zinc entry-exit experiment shown for *TEF1* strains. See additional examples in fig. S3. (**C**) Relative difference between wild-type and constitutive strains upon exit from starvation, shown as the fraction of wild-type to constitutive cells after recovery. Data are means ± SEM. See table S2 for number of repeats.

the media as well (to below our detection limit of 5 μM). This suggests that depletion of high-affinity transporters from cells in rich media benefits cells more during recovery from starvation than during entry into starvation.

We attributed the delayed recovery of the cells constitutively expressing the high-affinity transporters to their shortened preparation phase. We therefore predicted that this phenotype would be rescued by constitutively activating the early starvation program, rendering the cells constantly prepared. The phosphate starvation response is induced in two stages: first during intermediate limitation, and later during deep starvation (*24*). We reasoned that the first stage may constitute preparation and used a previously described *PHO4* allele [$PHO4^{SA1234}$ (*24*)] to constitutively activate this response in both the wild-type and $PHO84^{C}$ cells (*23*). In these cells, Pho4 is present in the nucleus even in conditions in which phosphate is abundant (Fig. 4, A and B). As predicted, this allele fully rescued the delayed recovery of the constitutive strains (Fig. 4, C and D, and fig. S5), strongly supporting our hypothesis that the delayed recovery of constitutive strains results from the shortened preparation of these cells.

Our results indicate that the dual-transporter motif enables cells to prepare for nutrient depletion and thereby improves their recovery once nutrients are replenished. How could early activation of the starvation program facilitate recovery? By measuring the gene expression profiles of cells as they depleted phosphate, we defined a large number of genes whose expression is induced in wild-type cells during the early starvation program but is delayed in cells that constitutively express the high-affinity transporters (Fig. 2D). Those genes are candidates for improving recovery. Of particular note are the genes *PHM2* to *PHM4* required for storage of phosphate in the vacuoles, as this storage plays a role during nutrient resupply (*25*).

Our work suggests that the low-affinity transporters function as signaling entities, allowing cells to sense a reduction in nutrient level before this reduction becomes limiting for growth. In principle, this function could be provided by extracellular receptors, but this would negate the advantages of directly monitoring intracellular nutrients (*15*, *26*–*28*). The dual-transporter system enables cells to combine internal and external sensing, benefiting from the respective advantages of both strategies.

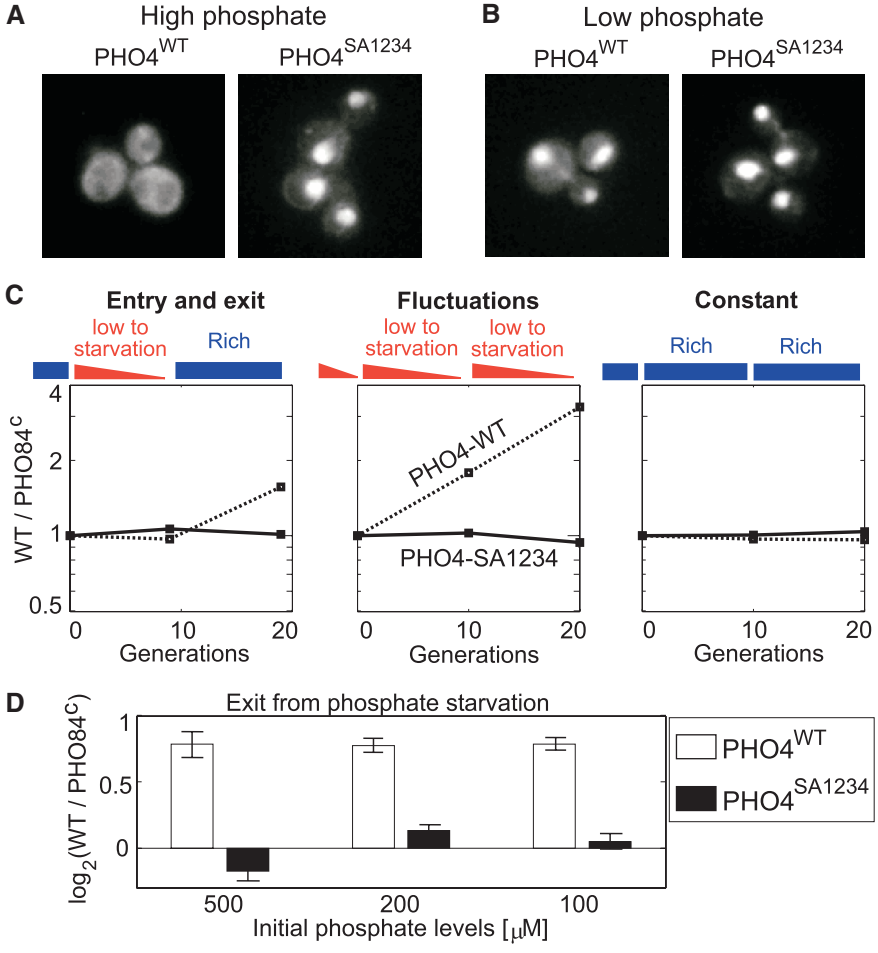

Fig. 4. Prolonged recovery of the $PHO84^{C}$ cells is rescued by constitutive activation of the intermediate-starvation program. (**A** and **B**) Nuclear localization of $PHO4^{SA1234}$. (**C** and **D**) Rescue of $PHO84^{C}$ by $PHO4^{SA1234}$. Competition assays are as in Fig. 3, B and C, with the $PHO84^{C}$ cells also expressing the $PHO4^{SA1234}$ allele. Data are means ± SEM. See table S2 for number of repeats. The entry phenotype was not rescued by $PHO4^{SA1234}$, which suggests that it does not result from prolonged preparation (fig. S5). Analogous rescue experiments in the zinc system were not possible because cells expressing an activated *ZAP1* allele have growth defects both in high and low zinc (not shown).

References and Notes

1. P. Daram *et al.*, *Plant Cell* **11**, 2153 (1999).
2. D. J. Eide, *Annu. Rev. Nutr.* **18**, 441 (1998).
3. D. J. Eide, *J. Biol. Chem.* **284**, 18565 (2009).
4. R. M. Harris, D. C. Webb, S. M. Howitt, G. B. Cox, *J. Bacteriol.* **183**, 5008 (2001).
5. P. F. Lasko, M. C. Brandriss, *J. Bacteriol.* **148**, 241 (1981).
6. K. H. Liu, Y. F. Tsay, *EMBO J.* **22**, 1005 (2003).
7. A. M. Marini, S. Soussi-Boudekou, S. Vissers, B. Andre, *Mol. Cell. Biol.* **17**, 4282 (1997).
8. U. S. Muchhal, J. M. Pardo, K. G. Raghothama, *Proc. Natl. Acad. Sci. U.S.A.* **93**, 10519 (1996).
9. B. L. Persson *et al.*, *Curr. Genet.* **43**, 225 (2003).
10. F. Santos-Beneit, A. Rodríguez-García, E. Franco-Domínguez, J. F. Martín, *Microbiology* **154**, 2356 (2008).
11. R. L. Seymour, V. Ganapathy, A. L. Mellor, D. H. Munn, *J. Leukoc. Biol.* **80**, 1320 (2006).
12. D. E. Townsend, B. J. Wilkinson, *J. Bacteriol.* **174**, 2702 (1992).
13. D. D. Wykoff, E. K. O'Shea, *Genetics* **159**, 1491 (2001).
14. H. I. Yamamura, S. H. Snyder, *J. Neurochem.* **21**, 1355 (1973).
15. S. Levy, N. Barkai, *FEBS Lett.* **583**, 3974 (2009).
16. C. Auesukaree *et al.*, *J. Biol. Chem.* **279**, 17289 (2004).
17. A. J. Bird *et al.*, *EMBO J.* **22**, 5137 (2003).
18. Y. S. Lee, S. Mulugu, J. D. York, E. K. O'Shea, *Science* **316**, 109 (2007).
19. W. Qiao, M. Mooney, A. J. Bird, D. R. Winge, D. J. Eide, *Proc. Natl. Acad. Sci. U.S.A.* **103**, 8674 (2006).
20. A. Mitchell *et al.*, *Nature* **460**, 220 (2009).
21. I. Tagkopoulos, Y. C. Liu, S. Tavazoie, *Science* **320**, 1313 (2008); 10.1126/science.1154456.
22. D. D. Wykoff, A. H. Rizvi, J. M. Raser, B. Margolin, E. K. O'Shea, *Mol. Cell* **27**, 1005 (2007).
23. See supporting material on *Science* Online.
24. M. Springer, D. D. Wykoff, N. Miller, E. K. O'Shea, *PLoS Biol.* **1**, e28 (2003).
25. N. Ogawa, J. DeRisi, P. O. Brown, *Mol. Biol. Cell* **11**, 4309 (2000).
26. T. Bollenbach, S. Quan, R. Chait, R. Kishony, *Cell* **139**, 707 (2009).
27. S. Levy *et al.*, *PLoS ONE* **2**, e250 (2007).
28. S. Zaman, S. I. Lippman, L. Schneper, N. Slonim, J. R. Broach, *Mol. Syst. Biol.* **5**, 245 (2009).

Acknowledgments: We thank S. Fialkov and S. Meizel for the technical help; D. Ben-Zvi, I. Soifer, and our lab members for helpful discussions; and E. O'Shea for the EB1264 plasmid. Microarrays data have been deposited in Gene Expression Omnibus (accession no. GSE32067). Supported by the European Research Council (IDEAS), NIH grant P50GM068763, and the Helen and Martin Kimmel Award for innovative investigations.

Supporting Online Material

www.sciencemag.org/cgi/content/full/334/6061/1408/DC1
Materials and Methods
SOM Text
Figs. S1 to S9
Tables S1 to S4
References (*29*–*35*)

18 April 2011; accepted 17 October 2011
10.1126/science.1207154

The Competitive Advantage of a Dual-Transporter System

Sagi Levy, Moshe Kafri, Miri Carmi and Naama Barkai

Science **334** (6061), 1408-1412.
DOI: 10.1126/science.1207154